Catalysis Today 169 (2011) 112–117

Contents lists available at ScienceDirect

Catalysis Today

journal homepage: www.elsevier.com/locate/cattod

Optimization of Cu doped ceria nanoparticles as catalysts for low-temperature methanol and ethylene total oxidation

R. Dziembaj*, M. Molenda, L. Chmielarz, M.M. Zaitz, Z. Piwowarska, A. Rafalska-Łasocha

Jagiellonian University, Faculty of Chemistry, Department of Chemical Technology, Ingardena 3 Str., PL-30-060 Cracow, Poland

ARTICLE INFO

Article history:
Received 11 June 2010
Received in revised form 28 October 2010
Accepted 2 November 2010
Available online 12 January 2011

The paper is dedicated to Professor Jerzy Haber, in memory of our Unforgettable Teacher and Master.

Keywords:
Ce–Cu oxide nanoparticles
Ceria catalysts
Reverse microemulsion method
VOC incineration

ABSTRACT

A series of Ce–Cu nanoparticle oxide catalysts were prepared by a modified reverse microemulsion method using a mixture of cerium and copper nitrate solutions and various precipitating agents ($(NH_4)_2CO_3$, NaOH or tetrapropylammonium hydroxide). The obtained precursors were transformed into the mono-phase oxide forms by calcination in air atmosphere. The catalytic activity of the $Cu_xCe_{1-x}O_2$ nanoparticles in the methanol and ethylene incineration depended on both copper loading and size of nanocrystallites. Optimal composition as well as morphology of the active catalytic Ce–Cu oxide systems were proposed.

1. Introduction

Liu and Flytzani-Stephanopoulos [1] indicated that Cu-doped ceria has better redox properties and oxygen storage capacity than those of pure ceria. Such properties favor the CuO–CeO_2 system (among the other oxide systems) to be applied in volatile organic compounds (VOCs) incineration instead of noble metal catalysts. The mixed oxide catalysts were initially prepared by an impregnation method, giving two- or multi-phase oxide systems. Better dispersion has been obtained using highly exothermic redox reactions, for example combustion of urea with nitric salts [2,3]. The mixed oxides obtained by this method showed segregation of CuO phase at higher copper contents [2–5]. The missing of CuO phase in XRD patterns of the samples with lower Cu concentration was ascribed to very fine dispersion of CuO particles [6,7] or to formation of solid state solution in CeO_2 phase [8]. Delimaris and Ioannides suggested formation of an interfacial solution, forming an outer layer on the particles [3].

The reverse microemulsion mediated technique for formation of nanosized particles proposed by Zarur and Jing [9] allows formation of nanosized particles more homogeneous than those obtained by the other methods. The structural and electronic properties of the $Cu_xCe_{1-x}O_2$ nanosystems prepared by a reverse microemulsion method were characterized by Rodriguez et al. [10] with synchrotron-based X-ray diffraction, X-ray absorption spectroscopy, Raman spectroscopy, and density functional calculations. The Rietveld refinement of the high-Q X-ray diffraction data indicates that Cu substitutes Ce in ceria lattice and coexists with O vacancies [10]. The copper ions occupying the Ce sites in the fluorite-type CeO_2 lattice are forced to reach the coordination number of 8. Such an unusual number of Cu ions causes strong structural distortions. The density functional calculations performed for bulk $Cu_xCe_{1-x}O_2$ by Rodriguez et al. [10] resulted in the statement that only 4 oxygen atoms are the closest neighbors, while the next two are in a distance of about 0.04 nm longer, and the other two even far away of about 0.11 nm. These strong structural distortions may explain the simultaneously observed slight increase in the lattice parameter and parallel formation of the oxygen vacancies with introduction of copper into CeO_2 lattice [11].

The surface layers of the $Cu_xCe_{1-x}O_2$ solid solution can be different from the bulk of this oxide system. The results of UV–vis diffuse reflectance spectroscopy showed mainly presence of the individually dispersed copper ions in the surface layers of $Cu_xCe_{1-x}O_2$, though oligonuclear $[Cu–O–Cu]_n$ species were present also but in the lower amounts [12]. Additionally, the calcination procedure follows to formation of grains from the nanosized precursors obtained by the microemulsion techniques. These grains show a porous structure which is not frequently characterized, though it is very important for establishment of the adsorptive and catalytic prop-

* Corresponding author. Tel.: +48 12 6632260; fax: +48 12 6340515.
E-mail addresses: dziembaj@chemia.uj.edu.pl, Roman.Dziembaj@gmail.com (R. Dziembaj).

0920-5861/$ – see front matter.
doi:10.1016/j.cattod.2010.11.061

erties of the mixed oxide catalysts. Such a difference in the pore structure of $Cu_xCe_{1-x}O_2$ obtained by microemulsion method using hydroxide or carbonate anions in the precipitation stage of the preparation was observed in our laboratory [12]. The agglomerates of $Cu_xCe_{1-x}O_2$ crystallites obtained with hydroxide agent formed the bottle-neck pores after calcinations with the uniform size distribution while the carbonate samples formed the non-uniform nanoparticles with slotted pores.

The catalysts based on the CuO–CeO_2 oxide system have been proposed as one of the best candidates for the preferential oxidation of CO in hydrogen rich reformate gas. Avgouropolos et al. [13] noted that these catalysts can act at temperatures as low as 100–200 °C, though small amounts of methanol play role of inhibitor in oxidation of both, CO and H_2 below 200 °C. The various catalysts based on the CuO–CeO_2 oxide system have been used for the incineration via total oxidation of various VOCs, e.g. ethanol [3], methanol [12,14], ethyl acetate [3], acetone and ethylene [12], benzene [15,16], toluene [3,15] and p-xylene [15]. In each case, the mixed oxide systems CuO–CeO_2 showed higher activity than both these oxides separately.

Our previous paper reported high catalytic activity of Ce–Cu oxide nanoparticles in the process of methanol, ethylene and acetone incineration [12]. It was shown than an increase in copper content in the range of 0–20 mole% resulted in a gradual activation of the catalysts in the VOC incineration. Additionally, it was proved that the method used for the catalysts synthesis strongly influenced the catalytic performance of the studied samples. The studies presented in this paper are a continuation of the mentioned above research. In order to determine the optimal composition of the catalysts the samples with copper content above 20 wt.% were studied and additionally, the influence of the size of catalysts nanocrystallites on their catalytic activity was determined.

2. Experimental

Three series of $Ce_{1-x}Cu_xO_2$, ($0 \leq x \leq 0.25$) nanostructured powders were obtained by a modified reverse microemulsion method [11], which differ each other by the used precipitation agents ($(NH_4)_2CO_3$, NaOH or tetrapropylammonium hydroxide (TPA)) and obtained intermediate precursors. A series C-Cu-X was obtained using $(NH_4)_2CO_3$ as precipitating agent and obtained product was in the form of carbonate precursor. Series H-Cu-X and T-Cu-X were obtained using NaOH and TPA as precipitating agents. In both these cases hydroxyl-oxide precursors were formed as products of precipitation. Two water-in-oil (w/o) microemulsions containing respectively 22 wt.% of the water phase, 48 wt.% of cyclohexane (POCh) as the oil phase and 30 wt.% of the surfactant (Triton X-100, Aldrich) and co-surfactant (n-hexanol, POCh) in weight ratio 2:1 were prepared. The appropriate mixtures of cerium ($Ce(NO_3)_3{\cdot}6H_2O$, POCh) and copper ($Cu(NO_3)_2{\cdot}6H_2O$, POCh) salts in the desired proportion were dissolved in the water phase of the first microemulsion. The water phase in the second microemulsion contained the solution of precipitating agent: $(NH_4)_2CO_3$ (POCh) for C-Cu-X series, NaOH (POCh) for H-Cu-X series and tetrapropylammonium hydroxide (TPA, AppliChem) for T-Cu-X series. The appropriate two transparent w/o microemulsions were carefully mixed together.

Precipitation of metal carbonates (series C-Cu-X) started few minutes after mixing of the microemulsions. The obtained precipitates were aging for 1 h under intensive stirring. When sodium hydroxide was used as a precipitation agent (series H-Cu-X) the resulting mixture had to be preserved at room temperature for 24 h under constant air flow. The observed changes in color indicated the end of the reaction. In the case of tetrapropylammonium hydroxide used as a precipitation agent (series T-Cu-X) the resulting mixture was treated with a small amount of 30% hydrogen peroxide (POCh) to accelerate oxidation of Ce^{3+} and precipitation of $CeO(OH)_2$. Next, the mixture was aging for 1 h under intensive stirring.

The resulting mixtures were separated by centrifugation and washed several times with acetone or mixture of acetone and water (1:1) providing a powder precursor. Finally, the powders were calcined under flow of air at 500 °C for 3 h. The optimal conditions of the calcinations processes were determined by the thermal analysis methods coupled with evolved gas analysis (EGA-TGA/DTG/SDTA) and published elsewhere [12].

The reference catalyst (called S-Cu-X series) was obtained by the wetness incipient impregnation method using solution of $Cu(NO_3)_2$ (POCh) and commercial CeO_2 powder (Aldrich). The calcination process was performed under a flow of air at 500 °C for 3 h.

The crystal structure of the obtained Cu-doped ceria nanoparticles were characterized by powder X-ray diffraction (XRD) in a *PW3710 Philips X'Pert* apparatus equipped with a graphite monochromator using Cu K_α ($\lambda = 0.154178$ nm) or Co ($\lambda = 0.178897$ nm) radiation. The average crystallite size (D_{XRD}) was calculated from the broadening of the following reflections (1 1 1), (2 0 0), (2 2 0) and (3 1 1) using the Sherrer method implemented in *Philips X'Menu Software*.

The surface morphology and the specific surface area of the obtained powders were evaluated from N_2 sorption measurements performed in a *Micrometrics ASAP 2010* using the BET isotherm method. About 500 mg of each sample was preliminary degassed at 250–300 °C for 4 h under pressure 0.26–0.4 Pa for 2 h. Than, N_2 sorption was performed at −196 °C. The average grain size was calculated from BET specific surface area with assumption of the spherical shape of grains and ceria crystallographic density of 7.2 g/cm^3.

The cerium based samples were tested as catalysts for the process of methanol and ethylene incineration. The catalytic experiments were performed under atmospheric pressure in a fixed-bed flow microreator system. Concentrations of the reactants and products were continuously measured using a quadruple mass spectrometer (*PREVAC*) connected directly to the reactor outlet. Prior to the catalytic test each sample of the catalyst (100 mg) was outgassed in a flow of pure helium at 450 °C for 1 h. The isothermal saturator (constant flow of helium, 0 °C) was used for the supplying of methanol into the reaction mixture, whereas ethylene was supplied from gas cylinder. The composition of gas mixture at the reactor inlet was [CH_3OH] = 0.5 vol.% or alternatively [C_2H_4] = 0.5 vol.%, [O_2] = 4.5 vol.% and [He] = 95.0 vol.%. The reaction was studied in the range from 100 to 600 °C with the linear temperature increase of 10 °C/min. Prior to the selection of such heating rate various temperature programs were tested (5, 10, and 15 °C/min). It was found, that there were not significant differences in the catalytic results up to 10 °C/min. The signal of the helium served as an internal standard to compensate possible small fluctuations of the operating pressure. The sensitivity factors of analysed mass-to-charge ratios (4, 12, 16, 17, 18 28, 30, 31, 32, 44) were calibrated using commercial mixtures of gases (1 vol.% C_2H_4 in He, 5 vol.% O_2 in He, 5 vol.% CO_2 in He). In the case of necessity, additional chromatographic analysis (*Varian 3400 CX*, packed columns: *Molecular Sieves 5A* and *Poropak Q*) was performed for identification of all the components of the outlet gases.

3. Results and discussion

The obtained materials were characterized by XRD measurements and the results are presented in Fig. 1. The XRD patterns revealed that the single phase solid solutions with fluorite-like structure were obtained for all the samples. For the samples of

Table 1
Structural and textural properties of the Cu-doped ceria obtained by microemulsion method and copper impregnated commercial CeO_2.

Sample	x in $Cu_xCe_{1-x}O_2$	BET surface area [m^2/g]	Total pore volume [cm^3/g]	Average pore diameter [nm]	Grain size, D_{BET} [nm]	Crystallite size, D_{XRD} [nm]
H-Cu-X series						
H-Cu-0	0	35.8	0.157	17.5	23.2	10.0
H-Cu-5	0.05	80.8	0.191	9.5	10.3	7.1
H-Cu-10	0.10	55.0	0.164	11.9	15.1	7.9
H-Cu-15	0.15	63.3	0.230	14.9	13.1	7.5
H-Cu-20	0.20	64.9	0.234	14.4	12.8	7.5
H-Cu-25	0.25	39.0	0.138	14.2	21.3	7.7
C-Cu-X series						
C-Cu-0	0	78.5	0.202	10.3	10.6	8.5
C-Cu-5	0.05	21.0	0.017	3.3	39.6	9.8
C-Cu-10	0.10	65.5	0.113	6.9	12.7	8.9
C-Cu-15	0.15	93.4	0.375	13.4	8.9	6.0
C-Cu-20	0.20	82.8	0.370	17.9	10.1	5.6
C-Cu-25	0.25	50.0	0.076	6.0	16.6	7.5
T-Cu-X series						
T-Cu-10	0.25	74.5	0.234	12.6	11.2	3.3
T-Cu-15	0.20	47.4	0.146	12.4	17.6	3.7
T-Cu-20	0.15	155.4	0.195	5.0	5.4	1.4
T-Cu-25	0.10	69.7	0.091	5.2	11.9	2.0

Sample	y Cu in yCuO/CeO_2	BET surface area [m^2/g]	Total pore volume [cm^3/g]	Average pore diameter [nm]	Grain size, D_{BET} [nm]
S-Cu-X series					
S-Cu-0	0	62.1	0.085	54.8	13.4
S-Cu-5	0.05	5.1	0.009	72.5	163.1
S-Cu-10	0.10	3.8	0.008	85.2	218.3
S-Cu-15	0.15	4.3	0.010	91.3	193.1
S-Cu-20	0.20	4.6	0.009	77.2	181.5

H-Cu-20 and H-Cu-25 the reflections at 35.5 and 38.8° 2theta, characteristic of the presence of CuO phase were found. However, the very small intensities of these reflections suggest only the presence of CuO traces. These reflections were not detected for the other studied samples. The average crystallite sizes (D_{XRD}), calculated using the Sherrer formula, are presented in Table 1. It could be seen that average crystallite size vary from l.4 to 10 nm depending on the precipitation method applied and are not affected by the Cu doping. It could be noted, that the application of Scherrer equation is limited for crystallite size below 3–5 nm. However, Scherrer method seems to be the most useful in qualitative determination of nanopowder crystallite size. Therefore, the value of 1.4 nm is rather an estimation (possibly determined with large error), but the obtained results (very wide maxima in powder diffraction patterns) clearly show that crystallites in a T-Cu-X series are smaller than in the other catalysts.

The results of textural measurements are presented in Table 1. The specific surface area of the samples obtained by the microemulsion method varies from 36 to 155 m^2/g. The analysis of the BET N_2-isotherms recorded for the obtained ceria samples reveals that in the case of carbonate (C-Cu-X) precursors the formation of the spherical grains (probably slightly agglomerated) is observed while for the ceria samples obtained from the hydroxy-oxides precursors (H-Cu-X and T-Cu-X) the bottle-like pores with the uniform size distributions are formed. Such a pore shape may be a result of the agglomeration of grains and/or crystallites. In consequence, the average grain size may be slightly larger than the average crystallite size, what is in accordance to the obtained experimental results (Table 1). For comparison the results of N_2-BET analysis of the copper impregnated CeO_2 support (S-Cu-X series) are shown. The BET surface area of pristine CeO_2 support was about 62 m^2/g, while deposition of 5% of CuO reduced the surface area to about 5 m^2/g. Further increase in copper loading did not result in significant changes of the surface area. Therefore, it could be concluded that copper oxide is deposited on the outer surface of ceria support and tightly fills the pores.

The $Cu_xCe_{1-x}O_2$ samples were tested in the role of catalysts for the incineration of methanol and ethylene. Carbon dioxide and water vapor were the only detected reaction products. The results of the methanol incineration over various ceria-based catalysts are presented in Fig. 2. The methanol conversion in a gas phase (without catalysts) started at temperature about 300 °C, whereas for the total combustion of alcohol the temperature of 500 °C was needed (Fig. 2a). The ceria-based catalysts significantly decreased the reaction temperature. Fig. 2a shows the results of the catalytic tests for a series of the samples obtained from carbonate precursors (C-Cu-X series). It should be noted that the catalytic activity of the samples gradually increases with an increase of the copper loading from 0 to 20%, whereas higher loading of this transition metal reduced the catalytic activity (C-Cu-25). The best results in this series of the catalysts were obtained for the C-Cu-20 catalyst, which was able to completely eliminate methanol from the reaction mixture at 275 °C.

Fig. 2b shows the results of methanol incineration for a series of catalysts obtained from the hydroxy-oxide precursors (H-Cu-X series). Similarly to the C-Cu-X series also for the H-Cu-X catalysts an increase of the copper loading in the range from 0 to 20 mole% activated the samples in the methanol incineration process. However, it should be noted that the catalytic activity of the sample with the copper loading of 25 mole% (H-Cu-25) is lower than that of H-Cu-20 and H-Cu-15.

The results of the methanol incineration for a series of catalysts precipitated with TPA (T-Cu-X series) are presented in Fig. 2c. Also in this case, an increase in the catalytic activity with an increase of the copper loading was found for T-Cu-10, T-Cu-15 and T-Cu-20 samples. The catalysts containing 25 mole% of copper (T-Cu-25) was significantly less active than T-Cu-20.

Therefore, the direct correlation between the copper loading and catalytic activity for all the studied series of the samples (C-Cu-X, H-Cu-X, T-Cu-X) exists only within transition metal contents up to 20 mole% of Cu. The further increase in copper content did not cause an increase of catalytic activity in VOC incineration or

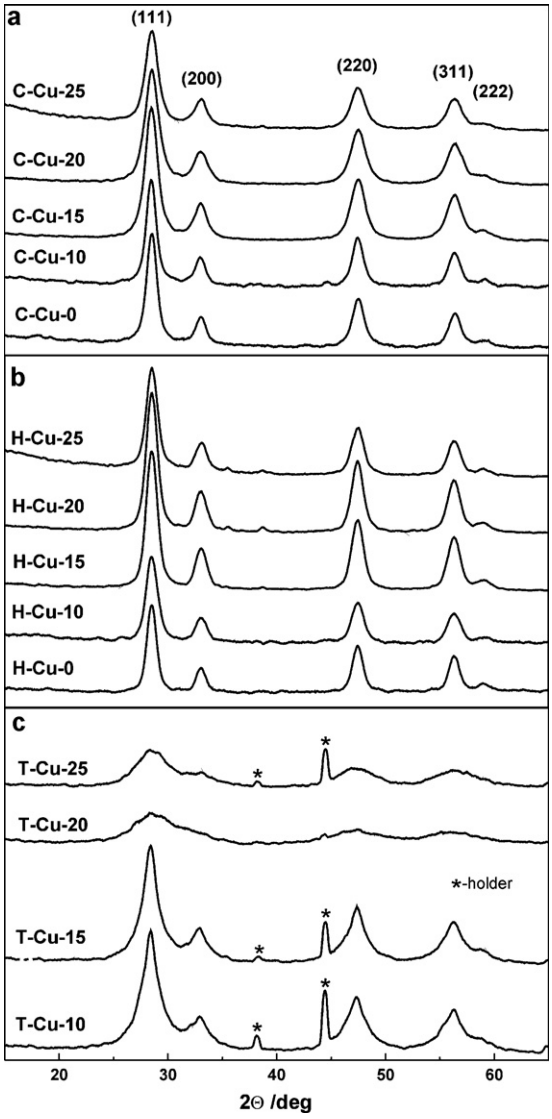

Fig. 1. XRD patterns of the Cu-doped ceria sample obtained by microemulsion method using $(NH_4)_2CO_3$ (a), NaOH (b) and tetrapropylammonium hydroxide (c) as precipitating agent.

even caused a fall of the activity. The best catalytic results were obtained for the sample H-Cu-20 produced from hydroxide precursors (H-Cu-X series), less active were catalysts obtained from carbonate precursors (C-Cu-X series), whereas the lowest activity was measured for the T-Cu-X series of the catalysts (precipitated with TPA).

The catalytic performances of the above described catalysts were compared with the results obtained for a series of the catalysts with the adequate copper loading (5–20 mole%) but obtained via impregnation of copper salt on the surface of commercial CeO_2 (S-Cu-X series). The impregnated catalysts did now show any meaningful differences between them (Fig. 2d), although their performances were poorer than the most active catalysts obtained by the microemulsion method (C-Cu-15, 20, 25 and H-Cu-15, 20). Therefore, it could be concluded that the loading value of copper deposited on the surface of ceria via impregnation is not a crucial parameter for determination of the catalytic performance in the methanol incineration process. This hypothesis is supported by the results of BET analysis of the samples obtained by the impregnation method. The BET surface area of pristine CeO_2 support was about 62 m^2/g, while deposition of 5% of CuO reduced the surface

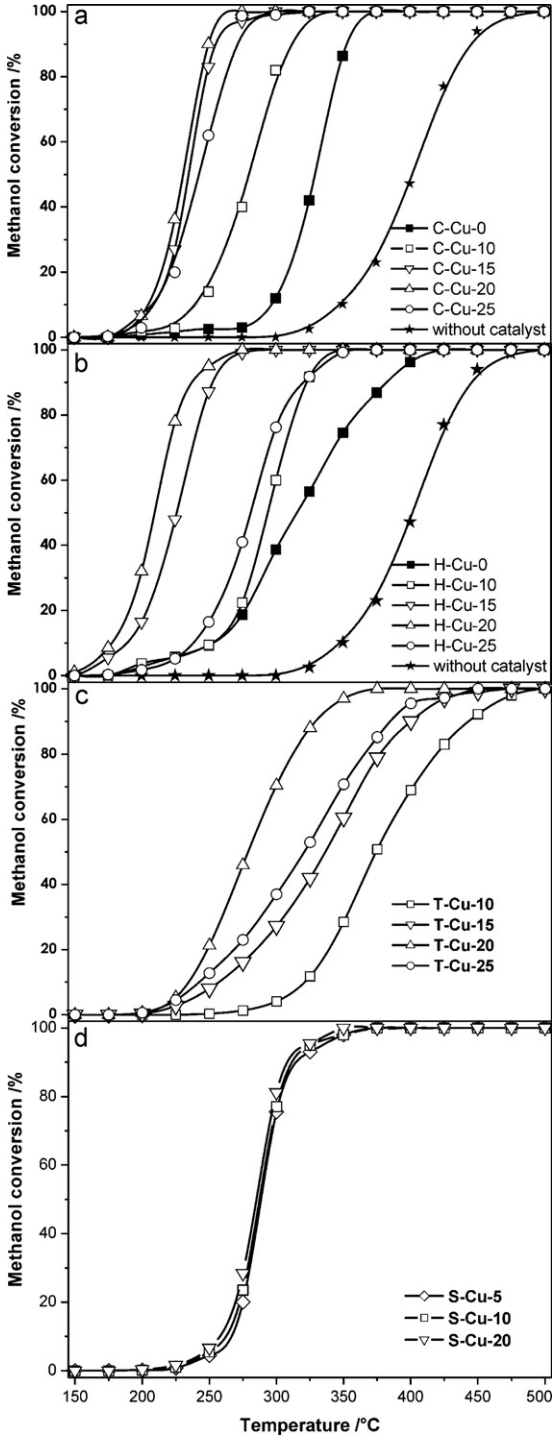

Fig. 2. The catalytic incineration of methanol on Cu-doped ceria based catalysts obtained from carbonate (a), hydroxy-oxides (b and c) and catalysts prepared by impregnation method (d).

area to about 5 m^2/g. Further increase in copper loading did not result in significant changes of the surface area. Textural parameters of a S-Cu-X (impregnated samples) series are presented in Table 1. Contrary to that, the $Ce_{1-x}Cu_xO_2$ catalysts obtained from microemulsion method showed clear but complex dependence on the copper loading. The difference between the series of Cu–Ce oxide catalysts can be explained by the formation of real solid state solutions in the case of the series of the microemulsion origin, while the impregnated series formed surface CuO species on the CeO_2 support or an interfacial solution, somewhat similar to proposed

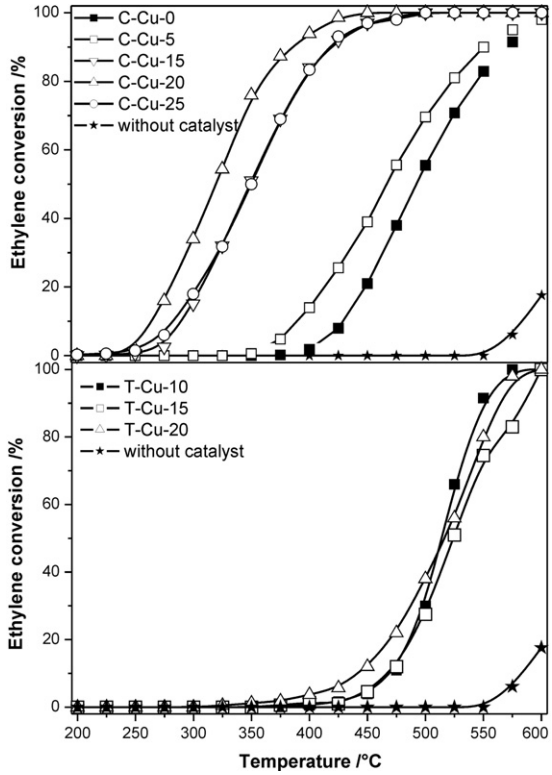

Fig. 3. The catalytic incineration of ethylene on Cu-doped ceria based catalysts obtained from carbonate (a) and hydroxy-oxides (b).

by Delimaris and Ioannides [3], but different from the bulk solution. According to the density functional calculations performed by Rodriguez et al. [10] for the Cu ion incorporation into the Ce positions in the CeO_2 bulk, this substitution caused strong lattice distortions which may cause much easier oxygen vacancies formation and metal ions reduction which both are important for the Mars van Krevelen mechanism of the redox catalysis. The role of the lattice oxygen as well as the other oxygen species in oxidative catalysis was introduced into discussions of the reaction mechanism in a classical review given by Bielański and Haber [17].

The ethylene incineration was studied using the series of C-Cu-X catalysts (obtained from carbonate precursors), which were found to be the most active ones. First of all it should be noted that combustion of ethylene needs considerably higher temperature comparing to methanol combustion. The reaction performed in the absence of any catalysts started at 550 °C (Fig. 3). The temperature of the ethylene incineration was significantly reduced for the process carried out in the presence of the C-Cu-X catalysts. Similarly, to the methanol incineration an increase of the copper loading in the range of 0–20 mole% gradually activated the catalysts, whereas the samples with higher transition metal loading (C-Cu-25) were less active than C-Cu-20.

Fig. 4, which summarizes the results of the catalytic tests performed for all the studied samples, shows that the optimal copper loading for the catalysts obtained by the microemulsion method is 20 mole%. Taking into account mentioned above observations it could be concluded that apart from the copper content there are also another features influencing the catalytic activity of the samples. It seems possible that the defect structure of ceria solid solution, which is a result of copper substitution, is an important feature influencing the catalytic performance. Substitution of copper into the cerium sub-lattice leads to the formation of oxygen vacancies, which may play an important role in the catalytic activation of the samples. Thus, the optimal concentration of oxygen vacancies as well as the defect structure, related to the highest activity of the catalysts, are formed in all the samples with 20 mole% of copper.

Different methods used for the preparation of the Ce–Cu catalysts resulted in their various crystallinity. The samples produced from carbonate (C-Cu-X series) and hydroxide (H-Cu-X series) precursors contained crystallites of average size in the range of 5.6–10.0 nm. Significantly smaller crystallites (below 3 nm) were produced for a series of the T-Cu-X samples (precursor precipitated with TPA). Fig. 5 shows the catalytic activity (presented as temperature needed for 50% of the methanol conversion) of the samples with 10 and 20% of the copper loading obtained by different methods as a function of the average crystallite size. It should be noted that larger crystallites of the $Cu_xCe_{1-x}O_2$ catalysts are significantly more active than smaller ones. Decrease of the catalytic

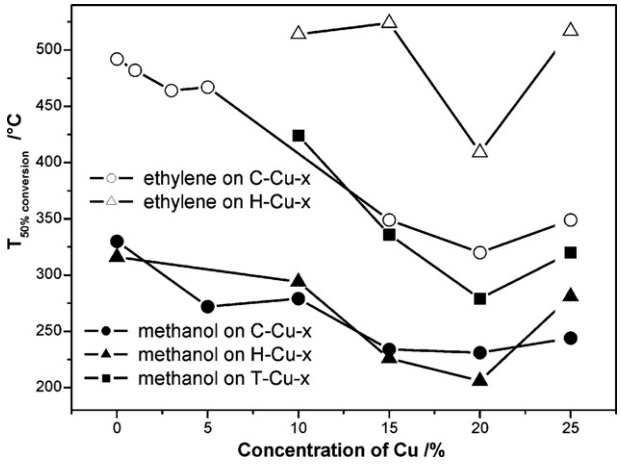

Fig. 4. The dependence of temperature necessary for 50% conversion of methanol or ethylene on copper content in Cu-doped ceria catalyst.

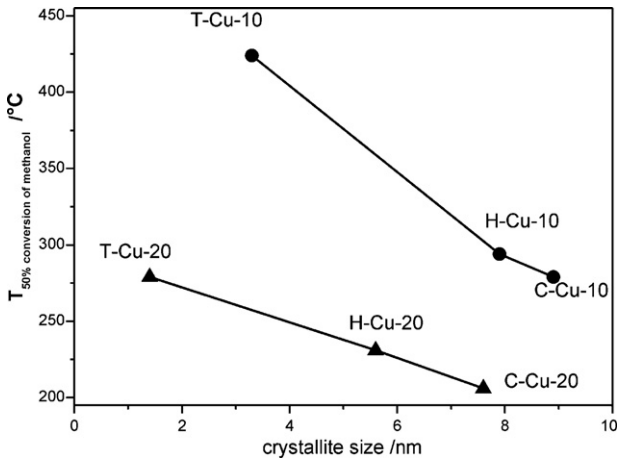

Fig. 5. The dependence of temperature necessary for 50% conversion of methanol on crystallites size of Cu-doped ceria catalyst.

activity observed for decreasing crystallite size could be explained by changes in the electronic and defect structure of the catalyst, which are a result of strong structural stress within nanocrystallites. It could be expected that such a stress, which is stronger for smaller crystallites, modifies their redox properties and the mobility of oxygen within nano-crystallites. Assuming that the process of methanol and ethylene proceeds according to the Mars van Krevelen mechanism (such a mechanism was proposed for incineration of various VOCs [e.g. 18, 19]) both these features determine the effectiveness of the catalytic reaction. This leads to the conclusion that transport phenomena in the bulk of the ceria catalyst must be taken into consideration. Moreover, it seems that bulk properties of the nano-catalysts are more important than the surface ones. The mobility of the oxygen ions as well as electronic transport properties within nano-catalyst crystallites seem to be limiting factors of their catalytic performance.

4. Conclusions

The reverse microemulsion method applied for synthesis of Cu–Ce oxide systems resulted in formation of nanocrystalline solid solutions with fluorite like structure characteristic of ceria. In the whole range of copper content (0–25 mole%) a single phase materials were successfully obtained. Various methods applied for the precipitation of ceria precursors gave a possibility to control the size of nanocrystallites. Nanocrystalline Cu–Ce oxide materials were found to be active catalysts of the methanol and ethylene incineration. However, activity of these catalysts strongly depended on their composition and crystallite size. It was shown that increase in copper loading in the range of 0–20 mole% resulted in gradual activation of the catalysts, whereas an increase in copper content into 25 mole% caused a significant decrease in the catalytic activity. Moreover, a correlation between catalytic activity and crystallite size was found. Decrease of crystallite size resulted in lower catalytic activity. Probably, both these effects are related to an optimal concentration of oxygen vacancies and an appropriate defect structure formed during substitution of copper into ceria lattice. Such vacancies and defect structure are necessary for an effective transport of oxygen ions as well as electrons within nanocrystallites.

Acknowledgment

This work has been financially supported by the Polish Ministry of Science and Higher Education under grant no. N N209 099337.

References

[1] W. Liu, M. Flytzani-Stephanopoulos, J. Catal. 153 (1995) 317–332.
[2] G.R. Rao, H.R. Sahu, B.G. Mishra, Colloids Surf. A 220 (2003) 261–269.
[3] D. Delimaris, T. Ioannides, Appl. Catal. B: Environ. 89 (2009) 295–302.
[4] G. Avgouropoulos, T. Ioannides, H. Matralis, Appl. Catal. B: Environ. 56 (2005) 87–93.
[5] M.F. Luo, J.M. Ma, J.Q. Lu, Y.P. Song, Y.J. Wang, J. Catal. 246 (2007) 52–59.
[6] P. Bera, S.T. Aruna, K.C. Patil, M.S. Hegde, J. Catal. 186 (1999) 36–44.
[7] S. Hocevar, U.O. Krasovec, B. Orel, A.S. Arico, A.H. Kim, Appl. Catal. B: Environ. 28 (2000) 113–125.
[8] P. Bera, K.R. Priolkar, P.R. Sarode, M.S. Hegde, S. Emura, R. Kumashiro, N.P. Lalla, Chem. Mater. 14 (2002) 3591–3601.
[9] A.J. Zarur, J.Y. Jing, Nature 403 (2000) 65–67.
[10] X. Wang, J.A. Rodriguez, J.C. Hanson, D. Gamarra, A. Martinez-Arias, M. Fernandez-Garcia, J. Phys. Chem. B 109 (2005) 19595–19603.
[11] M. Molenda, R. Dziembaj, L. Chmielarz, M. Drozdek, Z. Piwowarska, A. Rafalska-Łasocha, Polish J. Environ. Stud. 18 (2009) 151–154.
[12] R. Dziembaj, M. Molenda, L. Chmielarz, M. Drozdek, M.M. Zaitz, B. Dudek, A. Rafalska-Łasocha, Z. Piwowarska, Catal. Lett. 135 (2010) 68–75.
[13] G. Avgouropolos, J. Papavasiliou, T. Ioannides, Catal. Commun. 9 (2008) 1656–1660.
[14] R. Dziembaj, L. Chmielarz, M. Molenda, M.M. Zaitz, M. Drozdek, B. Dudek, Polish J. Environ. Stud. 18 (2009) 39–42.
[15] C.H. Wang, S.S. Lin, S.B. Liu, H.S. Weng, Chemosphere 65 (2006) 503–509.
[16] C. Hu, Q. Zhu, Z. Jiang, Y. Hang, Y. Wang, Micropor. Mesopor. Mater. 113 (2008) 427–434.
[17] A. Bielański, J. Haber, Catal. Rev.: Sci. Eng. 19 (1979) 1–41.
[18] C. He, P. Li, J. Cheng, Z.-P. Hao, Z.P. Xiu, Water Air Soil Pollut. 209 (2010) 365–376.
[19] S. Minicò, S. Sciré, C. Crisafulli, R. Maggiore, S. Galvagno, Appl. Catal. B 28 (2000) 245–251.